

## Epidemiology of *Vibrio* spp. in Coastal Waters Using ENVISAT/AATSR Satellite Data

C. Rodriguez-Benito<sup>1</sup>, M. Fea<sup>2</sup>, C. Haag<sup>3</sup>

### 1.1 Tele-Epidemiology, A Recent Discipline

In recent years a new discipline has been developed following the novel applications of modern Earth observation using satellite data. Spatial epidemiology, or tele-epidemiology, can be considered a secondary application of Earth observation data, used when a specific target cannot be measured directly using satellite imagery, but only detected through indirect methods (e.g. Scavuzzo and Fea, 2005). For example, an increase in sea surface temperature (SST) can sometimes contribute to an increase in phytoplankton production as well as an increase in the concentration of associated bacteria including *Vibrio* sp., thus increasing the risk of human infection (Colwell and Cleveland, 2008). For example, in 2004 two large outbreaks occurred along coastal regions in southern Chile where high water temperatures favoured higher levels of *Vibrio parahaemolyticus*. A number of severe gastrointestinal infections in humans were reported after consumption of contaminated shellfish, which had a significant economic impact on the shellfish aquaculture industry. Every year new cases of *Vibrio* intoxications are reported in this area and data from several years are mentioned in this case study. Rodriguez et al. (2005) established a relationship between satellite-derived sea surface temperature (SST) and *Vibrio* intoxications in the Chilean marine environment. This type of application has also been successfully applied in other areas (Laws, 2006).

This case study is based on the implementation of AATSR data from the European ENVISAT satellite in the southern part of Chile in 2004. Figure 1.1 shows the high correlation between SST and the number of infectious cases in the population caused by this species of bacteria (taken from a study conducted in 2008). The 2008 outbreak spurred the development of a strategic satellite-based early warning

<sup>1</sup>Department of oceanography, Mariscope. Puerto Montt (Chile) *Email address:* [oceanografia@mariscope.cl](mailto:oceanografia@mariscope.cl)

<sup>2</sup>University Sapienza de Roma, Italy

<sup>3</sup>Department of oceanography, Mariscope. Puerto Montt, Chile

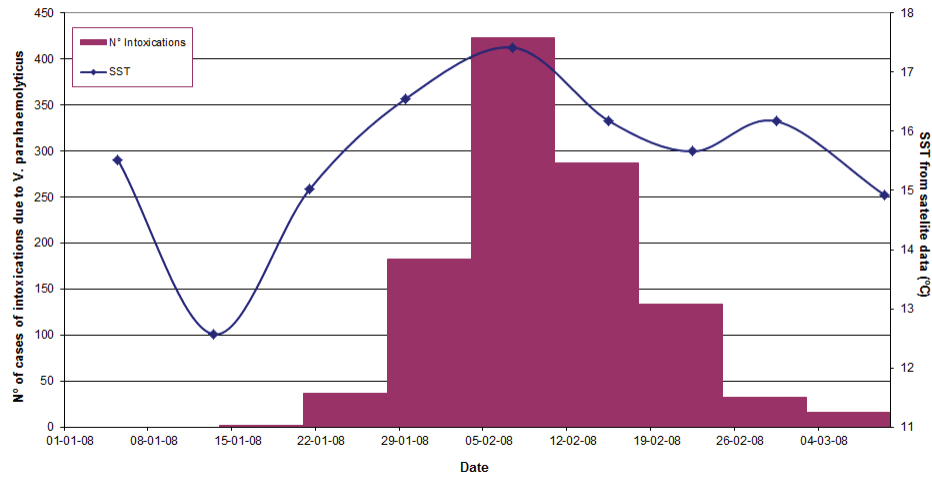


**Figure 1.1** Evolution of SST and number of intoxications, from a study that took place in 2008.

system to predict increases in the number of plankton-adhered *Vibrio* bacteria and to prevent the risk of consequent outbreaks of disease.

### 1.1.1 Description of the study area

The study area is located in the southern region of Chile, South America, at the beginning of the Chilean Patagonia. Reloncaví Bay and its adjacent fjords are semi-enclosed areas with a limited sea water exchange due to the coastal morphology and complex bathymetry (Figure 1.2). This bay has a significant freshwater input from the estuary formed by Petrohue and Puelo rivers, which carry the discharge from the mountains (Davila, et al., 2002). The Bay is 24 nautical miles long and 17 wide with a maximum water depth of 500 m at the entrance of the estuary and shallower waters near the coast.

The water interchange in this sound is much influenced by the circulation through the Chacao Channel, in the north of the main island, which determines an intense dynamic and is the origin of important gradients as the result of preliminary models implemented in the region (Figure 1.3) (Chambell, Haag, Rodriguez pers. comm.). Differences in sea water salinity in the bay are caused by the estuary and rivers that feed into the bay. Eastern areas have a much lower salinity (< 30) than western areas which are more influenced by subantarctic water with salinity values around 32.6. The average precipitation is around 1300 mm yr<sup>-1</sup> but rainfall amounts up to 2200 mm yr<sup>-1</sup> have been recorded in some areas, resulting in strong gradients and thermal fronts in the surface layers of the ocean (Silva and Guzman, 2006).

The principal circulation regime in this region is based on tidal forces, with a tidal range of around 7 m. The main water mass exchange occurs through the Gulf of Corcovado, flowing northwards during high tides and southwards during

low tides. Water flow is also influenced by the presence of several islands and bathymetric discontinuities. Due to the coastal morphology and bathymetry several physical features have been observed using remote sensing and local measurements, e.g. internal waves, gyres, local upwelling, and thermal fronts. Other features are observed both in and around channels, bays and islands that exhibit their own local dynamics.

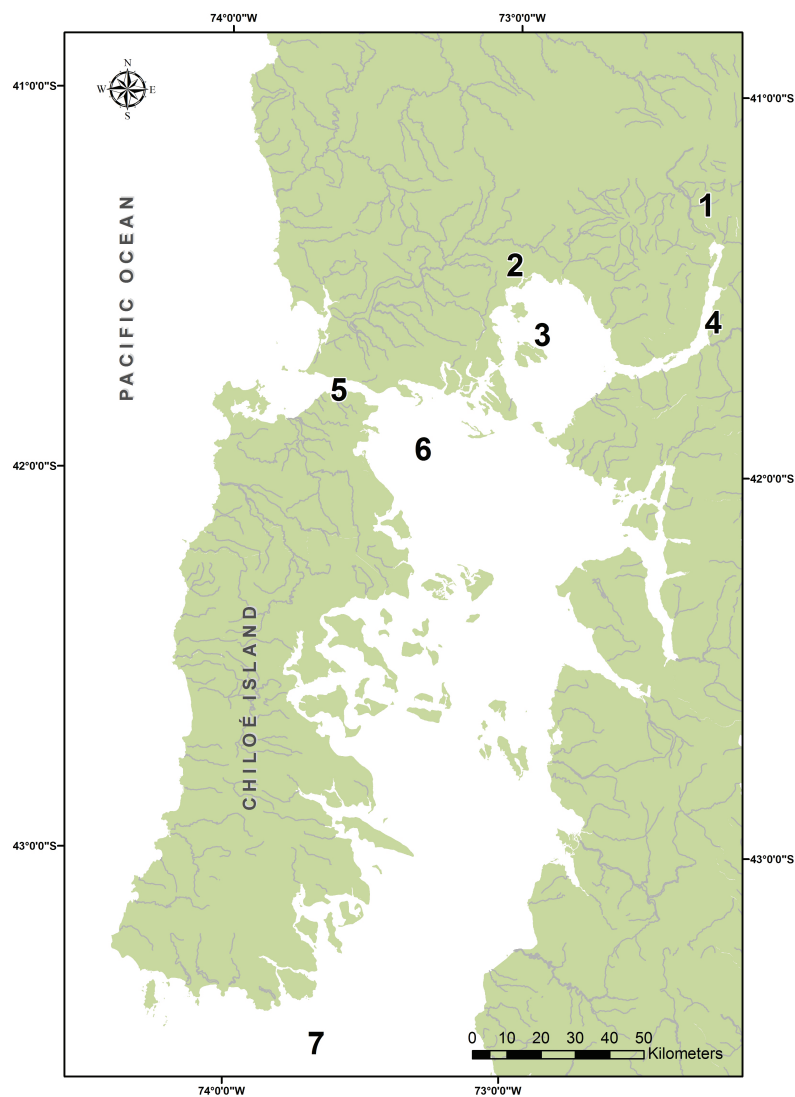


**Figure 1.2** Location of the study site in southern Chile, South America. 1. Reloncaví Estuary; 2. Puerto Montt; 3. Reloncaví Sound; 4. Puelo River; 5. Chacao Channel; 6. Gulf of Ancud; 7. Gulf of Corcovado

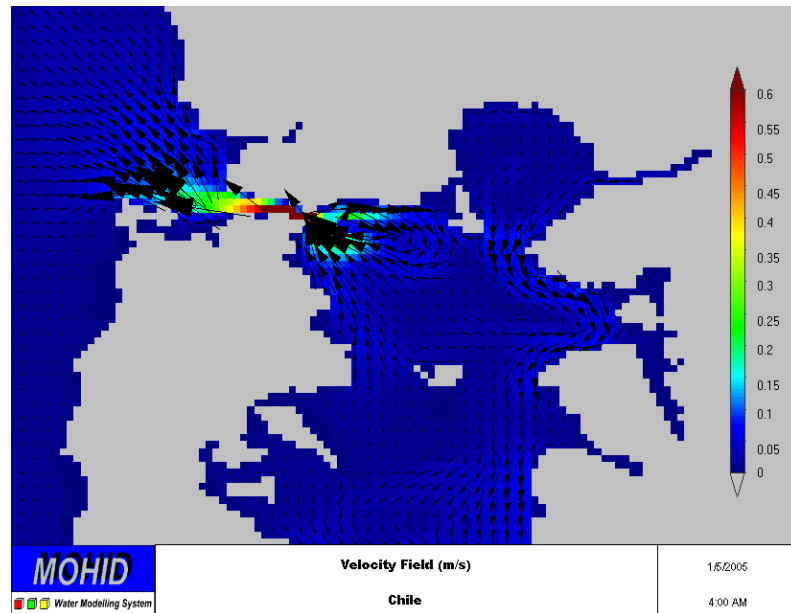


Figure 1.3 Circulation model using MOHID in the region of interest of this case study.

### 1.1.2 Socio-economic activities in southern Chile

Most of the population in this area lives in the city of Puerto Montt, located on the northern side of the Reloncaví Sound. Here, the aquaculture industry is responsible for a rapid increase in local population and urban development which has had a negative effect on conditions in the coastal environment, largely due to a lack of planning before the new district was established. Although Toledo et al. (2005) reported that the levels of faecal coliform bacteria remained relatively stable (with respect to reports from the previous 3 years), the number of coliforms was nevertheless above the accepted water quality values.

The greatest anthropogenic influence on the marine environment in this area is the local salmon aquaculture industry which discharges large amounts of organic material into coastal waters. In addition, the components of the fish food (colorants, antibiotics, vitamins, etc.) have had an impact on the biota and sediment composition over the last ~20 years. During July 2007, a large epidemiological outbreak occurred in this area as a result of the introduction of a non-endemic virus known as Infectious Salmon Anemia Virus (ISAV) which caused severe anemia of infected fish. Strong currents facilitated the rapid spread of the disease over several regions of Chile where the salmon farms are located (X<sup>th</sup> and XI<sup>th</sup> regions), forcing the cessation of all salmon farming activity for two years. Currently, the establishment of new environmental regulations have been implemented to mitigate the negative influence of the industry on the local environment, and to transform salmon farming into a long term, sustainable resource.

Another impact of human activity is related to tourist cruises, which arrive in Puerto Montt every year during the spring and summer months. The ballast water discharged from these ships can introduce foreign species into the local environment, and, if not pre-treated, could be a source of the pandemic strains.

The ecophysiological success of bacteria in the marine environment is highly dependent on salinity and temperature. This is true for *Vibrio parahaemolyticus*, which has a similar physiology to *V. cholera* of the same genus. It has been demonstrated that water temperature is one of the most important factors contributing to accelerated bacterial growth (Lobitz et al., 2000; Colwell and Cleveland, 2008). Monitoring SST is thus very important, not only because of the impact of climate change on the environment, but also because of the indirect effects of temperature on infectious diseases and human health.

### 1.1.3 Epidemiological case study

In 2003 an outbreak of a new bacteria for the area was identified in waters off the southern coastal region of Chile, between 41° and 43°S (centred at longitude 73°W). Not all strains of *Vibrio parahaemolyticus* cause illness; on the contrary, pathogenic strains represent a small percentage of the total *Vibrio parahaemolyticus* present in the environment or seafood (FDA, 2005). The outbreak on which this case study was based, was dominated by the pandemic strain O3:K6 (Gonzalez-Escalona et al., 2005). This strain has been reported as the most resistance to high water temperature (Andrews et al., 2003). One species, identified as *Vibrio parahaemolyticus*, is known to be harmful to humans, especially children and the elderly. Exposure to the bacteria is usually through the consumption of raw shellfish, which is a tradition in this area, although the risk of infection is greatly reduced if the shellfish are boiled for several minutes. This particular species of bacteria was the cause of more than 1,500 poisonings during the summer of 2004 in a region generally characterised by relatively cold water (< 15°C in summer, Tello and Rodríguez-Benito, 2009). In addition to the impact on public health, this outbreak also had economic and social repercussions. This region is one of the main shellfish harvesting areas in Chile and the industry had to be closed by the local authorities during the outbreak.

Several investigations have demonstrated that the main environmental factor for the prevalence of *Vibrio parahaemolyticus* is the water temperature (EPA 2005; Huq et al., 2005; De Souza et al., 2010) although for other areas salinity has been also mentioned as a critical factor in other regions (Martinez-Urtaza et al., 2008). This should be considered when the bacteria has been detected previously in the water, and if the toxin analysis in the shellfish determines its presence. It is important to mention that this species is a natural inhabitant of marine environments in coastal areas and estuaries worldwide (FAO/WHO, 2011). The optimal environmental conditions for the development of *Vibrio* spp. are related to an increase in air and water temperatures. Empirical evidence suggests that species of *Vibrio* have a

wide tolerance range of temperatures for optimal growth, but Kaneko and Colwell (1973) found that water temperatures in the range of 14° to 19°C are critical in the annual cycle of this species. Concentrations of *Vibrio parahaemolyticus* showed a marked increase when the water temperature rose to 19°C. Tello and Rodriguez (2009) demonstrated that SST had a positive anomaly of 1° to 2°C between 2003 and 2005 in the northern part of the inner region, which could have triggered the *Vibrio* outbreaks. This observation led to the use of satellite SST data as a tool for developing an early warning system for outbreaks of this toxic bacteria.

SST data from the AATSR (Advanced Along-Track Scanning Radiometer) sensor on ESA's ENVISAT satellite demonstrate an increase in sea surface temperature every summer in the region of interest. During January 2004, satellite and auxiliary data permitted the identification of those areas with the highest sea surface temperatures, and thus the highest probability of *Vibrio* spp. outbreaks and associated potential for human infection through the consumption of contaminated sea food such as shellfish. Regional health authorities used this information as well as auxiliary data to determine areas at risk for intoxication and took appropriate measures (Rodriguez et al., 2005). Since SST is directly correlated to bacterial growth, it can be implemented into routine monitoring of ocean health and environmental risk assessment.

New opportunities in the field of remote sensing will improve epidemiological applications. The launch of hyperspectral sensors and geostationary satellites equipped with instruments for measuring SST can extend the range of operational applications in this area.

## 1.2 Demonstration Section

### 1.2.1 Material and methods

SST data from ESA's AATSR instrument was used for this case study but MODIS-Terra and MODIS-Aqua data could also be used for comparison. ESA is responsible for the distribution of ENVISAT data which can be used for scientific or commercial purposes. For the latter, users should contact associated companies such as Eurimage and Spotimage. For scientific applications, data can be obtained free of charge by submitting a proposal to ESA. Data can be obtained through ftp or disc and in some cases, data at low resolution is distributed through the internet (see <http://earth.esa.int>; <http://envisat.esa.int> and [http://www.esa.int/Our\\_Activities/Observing\\_the\\_Earth](http://www.esa.int/Our_Activities/Observing_the_Earth)).

Level 2 data were used in this case study. The standard file name of the AATSR product is ATS\_NR\_2P (full resolution geophysical product), indicating the type of data format product and the processing level (2). For more information on the AATSR data products please refer to: <http://envisat.esa.int/handbooks/aatsr/CNTR1.htm#eph.aatsr.ug>. The processing software used is VISAT, part of the group

of tools in BEAM, an open-source toolbox and development platform for viewing, analysing and processing remote sensing raster data, developed by Brockmann Consultants for ESA (see <http://earth.esa.int/resources/softwaretools/>).

The Envisat data used in the demonstration section of this case study is a subset of a file acquired on 15 February 2010, which can be downloaded from the IOCCG website at: <http://www.ioccg.org/handbook/Rodriguez/>. This is metadata obtained in the N1 format. The original N1 file was reduced in size and saved as a BEAM-DIMAP file. The following links are recommended for becoming more familiar with these satellite data:

- ❖ <http://earth.esa.int/object/index.cfm?fobjectid=1462>
- ❖ [http://www.noc.soton.ac.uk/bilko/envisat/13\\_ats/start.html](http://www.noc.soton.ac.uk/bilko/envisat/13_ats/start.html)

### 1.2.2 Steps for processing satellite data using VISAT:

**Step 1:** Install VISAT (download from <http://earth.esa.int/resources/softwaretools/>).

**Step 2:** Open a new image through the menu option: "file ⇒ open data products". In a new window (on the left) select SST nadir metadata.

**Step 3:** Rotate the image vertically and/or horizontally since the satellite acquisition is made in ascending mode. This function is available with the option "Data flip" in the Tool menu (Figure 1.4).

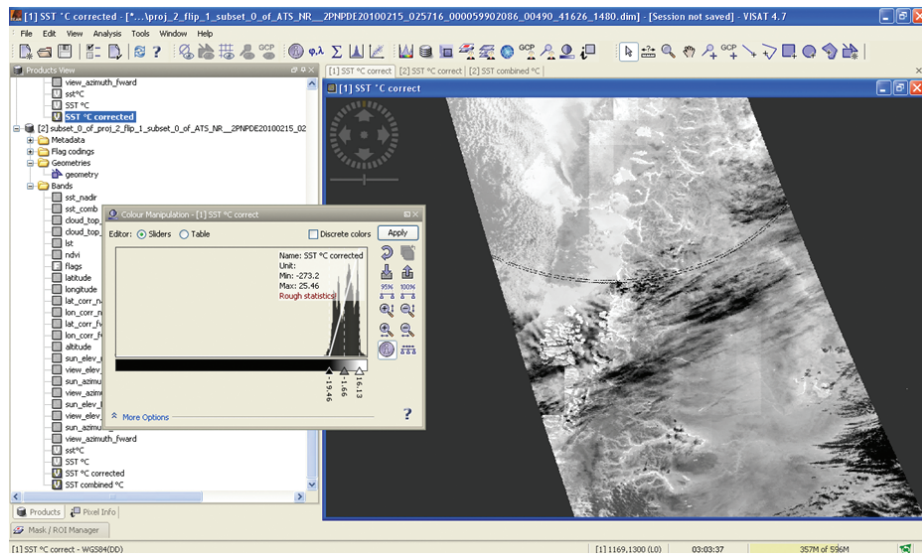


**Figure 1.4** An example of opening, flip and land mask over the image.

**Step 4:** Create a new product with a projected reference coordinate system (PCS) to work with data in the standard system. This step will be carried out with the

"Reprojection tool".

**Step 5:** Open layer manager and apply the land mask to clearly distinguish between land and ocean. Apply the cloud mask and select 0 as the percentage transparency. In the latest version of BEAM (2010) the land mask can be selected from other sources, such as other image files or ESRI shape files (Figure 1.5).

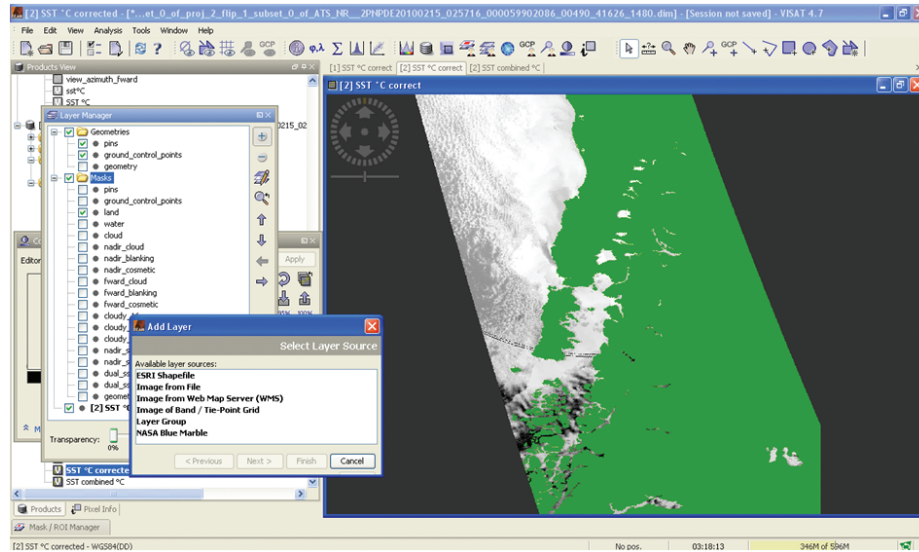


**Figure 1.5** Image colour manipulation and enhancements tool for an image from summer 2010.

**Step 6:** Create a new band to obtain the SST file in degree Celsius ( $^{\circ}\text{C}$ ). SST Envisat data are expressed in degree Kelvin ( $^{\circ}\text{K}$ ). Apply the following formula:  $\text{SST}_{\text{nadir}} - 273.17$ , to get a new SST nadir band in  $^{\circ}\text{C}$ .

**Step 7:** Compute a data histogram to stretch the colour palette of the SST band in  $^{\circ}\text{C}$ .

**Step 8:** Apply colour look-up-table (LUT) and improve the visualization of the temperature range by using a range of SST suitable for your particular area of interest. For example, in the southern region of Chile normal SST ranges are  $9^{\circ}$  to  $18^{\circ}\text{C}$  in summer and  $6^{\circ}$  to  $15^{\circ}\text{C}$  in winter.

**Step 9:** Mask pixels classified in a predetermined SST range that might present a high risk (Figure 1.7). For example, for the January 2004 AATSR image we created three masks: high risk:  $\text{SST} > 16^{\circ}\text{C}$ ; medium risk:  $14 < \text{SST} < 16$ ; lower risk:  $\text{SST} < 14$ .

**Step 10:** Create polygons for each risk area and export to a risk map using the region of interest (ROI) manager to rasterize a region of interest and export the selected pixels to other formats. Two such polygons are shown in Figure 1.7.



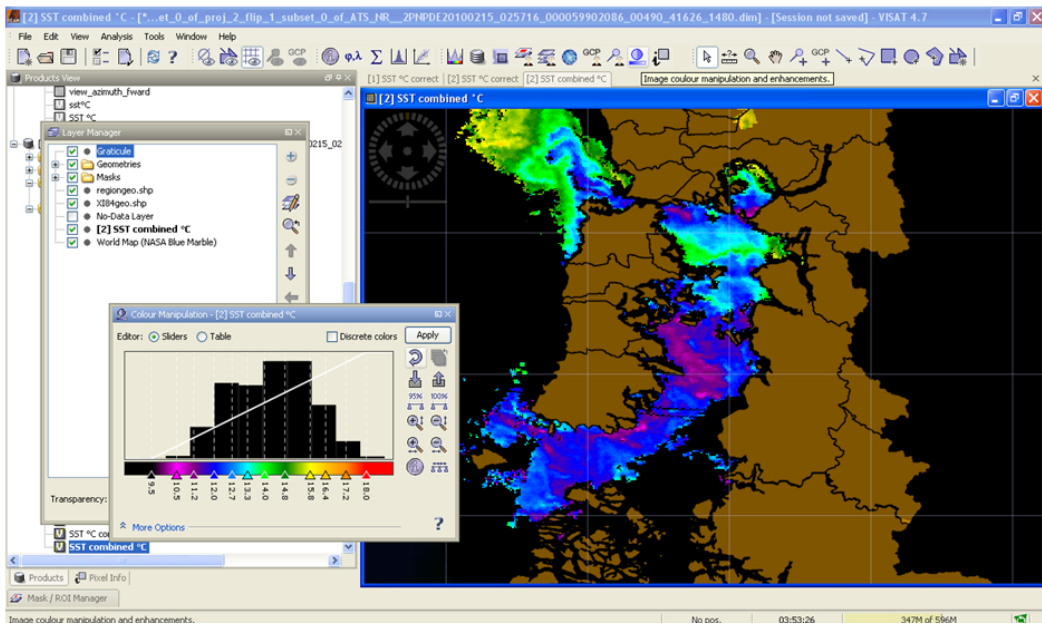


Figure 1.6 Applying LUT table to improve the visualization of the SST gradient.

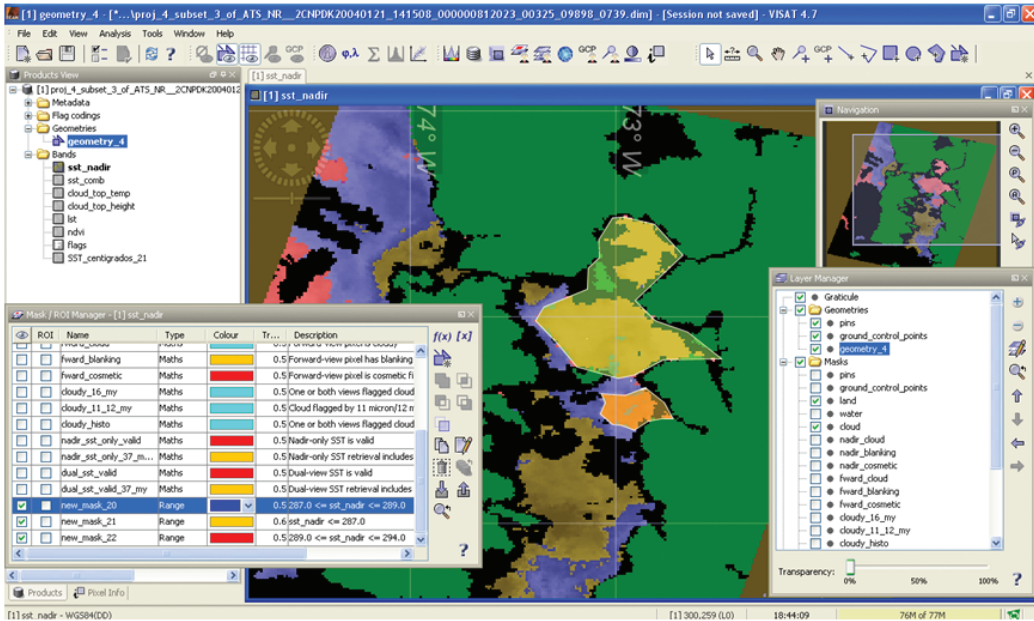


Figure 1.7 Creating regions of interest (ROIs) to export to GIS.

### 1.3 Training and Questions

**Q1:** Distinguish the three most vulnerable areas for toxic bloom conditions using the SST map from the AATSR image of 21 January 2004 (Figure 1.9), and formulate a hypothesis about the reason for their location.

**Q2:** Taking into account the described environment, which area has the highest risk for developing high concentrations of pathogens in the summer months, based on SST observations.

**Q3:** Determine the location of the major fronts in this coastal area from Figure 1.9 (2004). What factor(s) could be the key producers of these fronts.

**Q4:** What are the possible ecological effects of the fronts caused by the oceanographic dynamics in these areas? Several thermal fronts can be determined in Figure 1.8.

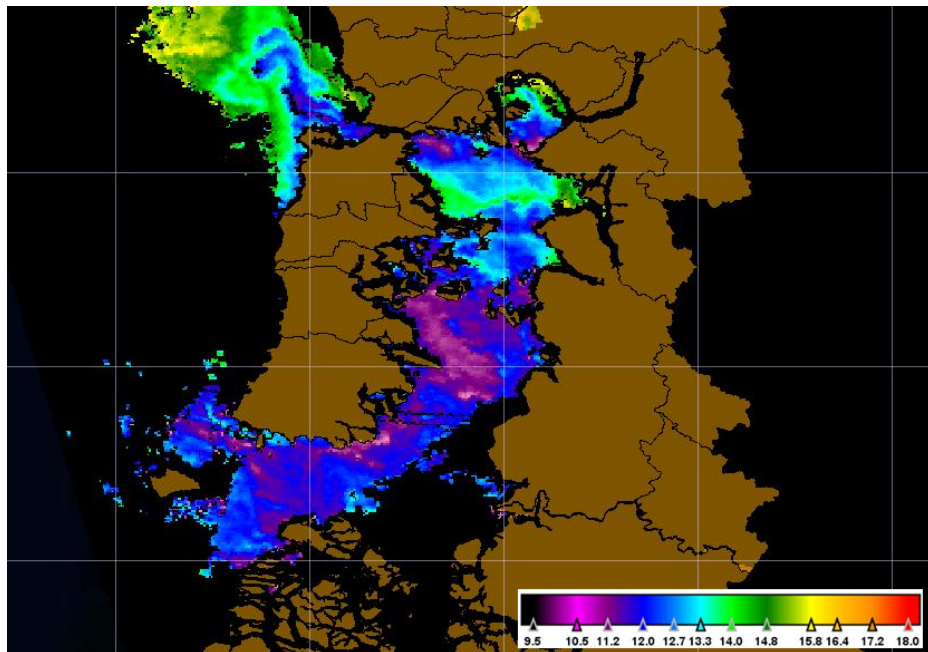


**Figure 1.8** SST data of 15 February 2010 demonstrates the interannual variability, as SST was lower than during other years. Thermal fronts demonstrate the natural barriers which can be found in this highly dynamic oceanographic region.

**Q5:** Using the results shown in Figure 1.10, on which date would you implement an early warning system and relay the necessary information to the local authorities to prevent potential poisonings due to the presence of toxic organisms in the coastal waters?

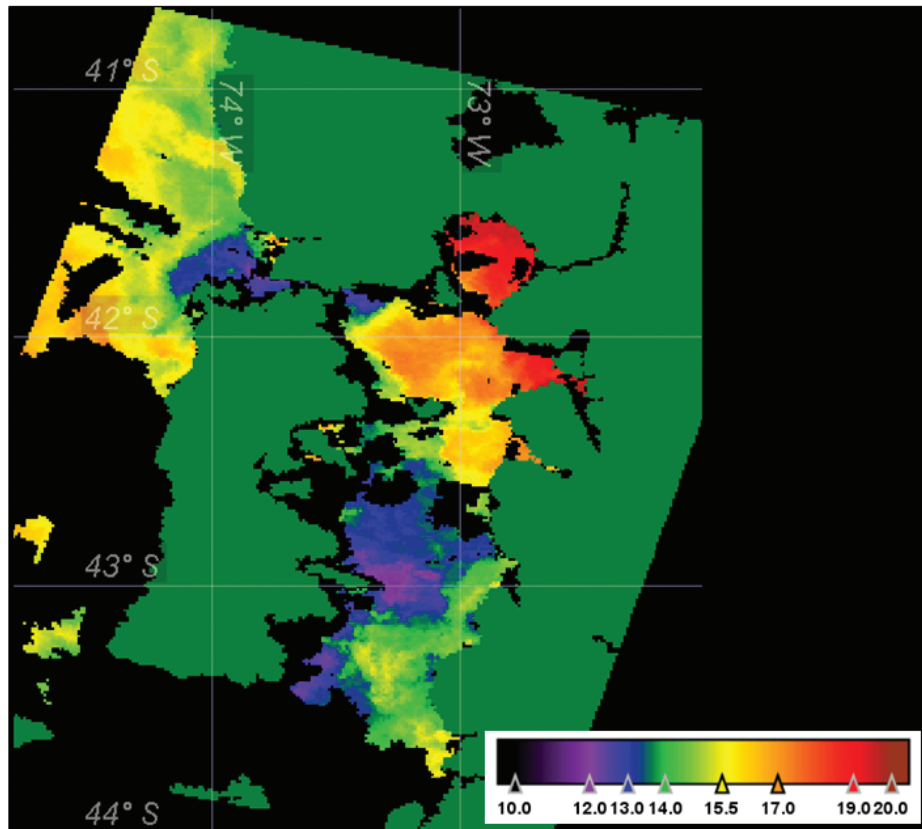


Figure 1.9 SST over the region of interest in January 2004.

**Q6:** Looking at the geomorphology of this region, which areas would you deem to be the danger zones that would facilitate exponential growth of toxic organisms?

## 1.4 Answers

**A1:** The three areas of interest would be:

1. Northern area: between parallel 41 and 42: Seno de Reloncaví and Golfo de Ancud.
2. Central area located in the inner part of Chiloé Island.
3. Gulf of Corcovado.

The vulnerability in these areas is related to circulation patterns, water mass exchange and the topography of this region. The first area, Reloncaví Bay, has very poor seawater exchange through its southern passage (Paso Nao), which inhibits the complete renewal of the water during each tidal cycle. Additionally strong fresh water input from the Reloncaví Estuary creates strong physical gradients due to differences in the temperature and salinity of the water masses. The second area is

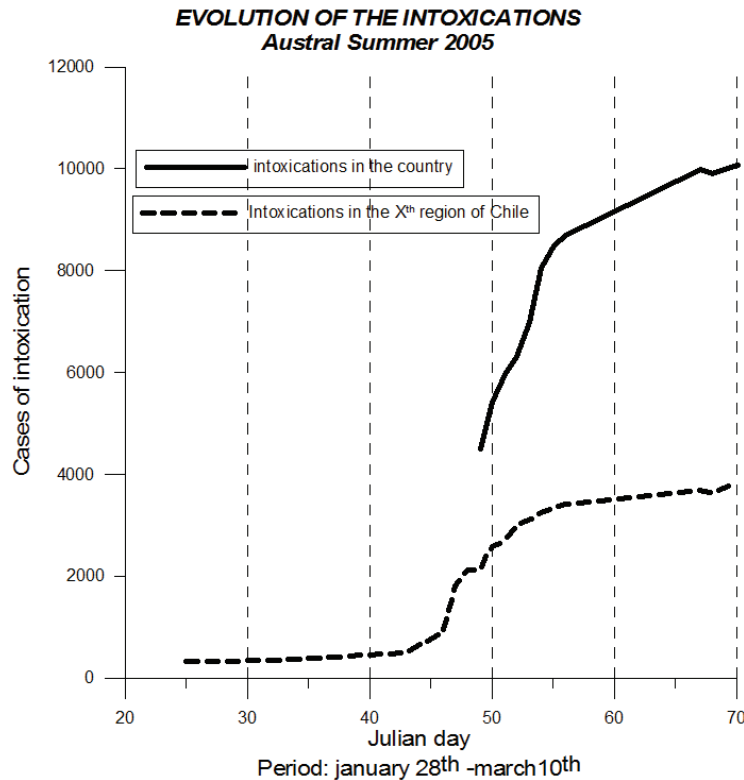


**Figure 1.10** Number of intoxications over the course of the austral summer in 2005 (which can be related to the increase in sea surface temperature).

largely influenced by tidal circulation and by the entry of water through the Chacao Channel. The circulation in this area is counter clockwise due to the Coriolis effect. The tidal circulation creates a so-called amphidromic system (Dietrich et al., 1975). Therefore algal bloom events are initiated on the eastern side and move towards the western side along with the main flow of water, thereby transporting potential bacterial pathogens. The third area is influenced by strong water mass exchanges with the open ocean through the Corcovado channel. This permanent exchange results in a lower water temperatures.

**A2:** The area where there is less water mass exchange and high stratification is the one at highest risk for the development of pathogens. The influence of the bathymetry and island barrier on tidal current flow in the north of Corcovado Gulf determines the dynamics of water mass exchange.

**A3:** The locations of the main fronts are:

1. The western area of the Gulf of Ancud caused by the input from the open ocean which mixes with the fresh water from river discharge.
2. The eastern area of the Gulf of Ancud resulting from the freshwater discharge

from the Reloncaví Sound.

3. South of this Gulf due to the local geomorphology, changes in the bathymetry and the presence of several islands.
4. Several fronts are observed in the Gulf of Corcovado: in the eastern part the front is due to the strong tidal flow, while in the western part the fronts develop for a number of reasons, one of which is the presence of internal waves which have been observed using radar data.

In summary, the origin of these fronts is determined primarily by the discharge of fresh water from the river and estuarine-plumes, the local bathymetry, geomorphology and tidal circulation.

**A4:** Fronts are formed at the edge of the river where estuarine plumes arise from freshwater mixing with salt water resulting in a halocline. The lower density, less saline water is carried by gravity seaward and covers the higher density seawater, forming fronts. These areas are marked by lines of foam and by sharp changes in the color of the water. Evidence suggests that these fronts are sites of enhanced biological activity, where phytoplankton and fish tend to aggregate (Mann and Lazier, 1996). The less saline water carries a high concentration of nutrients. The nutrients enrich these areas and thereby increase primary productivity. In addition, estuarine waters are often highly productive because nutrients upwelling from deeper waters become entrained (Lalli and Parsons, 1997).

**A5:** An early warning system should be implemented 6 -10 days before the event. If an early alarm system is established, this time frame would give local authorities enough time to activate a public alert and to protect the population from the potential risk of infection.

**A6:** The presence of numerous channels among the islands increases the velocity of the tidal currents. Future studies using radar data and hydrodynamic models are expected to corroborate this phenomenon.

## 1.5 References and further reading

- Andrews L, DeBlanc S, Veal CD, Park DL(2003) Response of *Vibrio parahaemolyticus* 03:K6 to a hot water/cold shock pasteurization process. Food Addit Contam 20(4):331-334.
- Colwell R, Cleveland C (2008) Global climate and health: predicting infectious disease outbreaks. In: Encyclopedia of Earth. Eds. Cutler J. Cleveland (Washington, D.C.: Environmental Information Coalition, National Council for Science and the Environment)
- Davila PM, Figueroa D, Muller E (2002) Freshwater input into coastal ocean and its relation with the salinity distribution off austral Chile (35°-55°S). Cont. Shelf. Res. 22 (3): 521-534.
- Dietrich G, Kalle K, Krauss W, Siedler G (1975) Allgemeine meereskunde. Ein Einführung in die Ozeanographie. Gebrüder Borntraeger. Berlin. 593pp.
- FAO/WHO [Food and Agriculture Organization of the United Nations/World Health Organization]. (2011). Risk assessment of *Vibrio parahaemolyticus* in seafood: Interpretative summary and Technical report. Microbiological Risk Assessment Series No. 16. Rome. 193pp.

- FDA (2005) Quantitative risk assessment on the public health impact of pathogenic *Vibrio parahaemolyticus* in raw oysters. FDA, Washington, DC.
- Gonzalez Escalona N, Cachicas V, Acevedo C, Rioseco ML, Vergara JA, Cabello F, Romero J, Espejo R (2005) Emerging Infectious Diseases 11(1): 129-131.
- Huq. A., R. Bradley Sack, Azhar Nizam, Ira M. Longini, G. Balakrish Nair, Afsar Ali, J. Glenn Morris, Jr., M. N. Huda Khan, A. Kasem Siddique, Mohammed Yunus, M. John Albert, David A. Sack, and Rita R. Colwell (2005) Critical Factors Influencing the Occurrence of *Vibrio cholerae* in the Environment of Bangladesh. Applied and environmental microbiology, Aug. 2005, 4645-4654 Vol. 71 (8): 4645-4654.
- Kaneko T, Colwell R (1973) Ecology of *Vibrio parahaemolyticus* in Chesapeake Bay. Journal of Bacteriology: 113 (1): 24-32.
- Martinez-Urtaza J, Lozano-Leon A, Varela-Pet J, Trinanés J, Pazos Y, Garcia-Martin O. (2008) Environmental determinants of the occurrence and distribution of *Vibrio parahaemolyticus* in the rias of Galicia, Spain. Appl. Environ. Microbiol. 2008; 74(1):265-74.
- Lalli C, Parsons T (1997) Biological Oceanography. An Introduction. 2nd Edition. The Open University, 314pp.
- Laws E (2006) Case study: Cholera. Oceanography 19 (2): 81-83.
- Lobitz B, Beck L, Huq A, Wood B, Fuchs G, Faruque ASG, and Colwell RR (2000) Climate and infectious disease: use of remote sensing for detection of *Vibrio cholerae* by indirect measurement. Proc Natl. Acad. Sci. USA 97 (4): 1438-1443.
- Mann KH, Lazier JRN (1996) Dynamics of marine ecosystems. Biological physical interactions in the oceans. 2nd Edition. Blackwell Science Inc. 394pp.
- Paulo de Souza Costa Sobrinho, Maria T. Destro, Bernadette D. G. M. Franco (2010) Correlation between Environmental Factors and Prevalence of *Vibrio parahaemolyticus* in Oysters Harvested in the Southern Coastal Area of Sao Paulo State, Brazil and Mariza Landgraf. Applied and Environmental Microbiology, Feb. 2010, p. 1290-1293
- Tello GA, Rodriguez-Benito C (2009) Characterization of mesoscale spatial-temporal patterns and variability of remotely sensed Chl a and SST in the Interior Sea of Chiloe (41.4-43.5°S). Int. J. Rem Sens, 30 (6): 1521-1536.
- Toledo H, Hernandez C, Rodriguez C, Bittner V, Ferreira L, Orellana F (2005) Study of monthly and seasonal faecal contamination in the coastal area adjacent to the submarine wastewater diffuser in the bay of Puerto Montt. Gayana 69 (1): 104-112.
- Rodríguez Benito C, Haag C, Vicente P, Fea M, Steffens H (2005) Monitoreo del fitoplancton en la costa sur de Chile mediante datos del instrumento MERIS de ENVISAT y observaciones in situ, Revista SELPER 23: 46 - 57.
- Scavuzzo CM and Fea M (2005) International Workshop on space technologies applies to human health for the benefit of Latin American and Caribbean countries-some highlights. Revista SELPER, Special edition 2005: 5-7
- Silva, N., D. Guzman. (2006). Physical and chemical characteristics between Boca del Guafo and Aysen Fjord (CIMAR 7 Fiordos Cruise). Cienc. Tecnol. Mar, 29 (1): 25-44.